ADVANCED OPTICAL MATERIALS
www.advopticalmat.de

Tunneling in Persistent Luminescence

Hei-Yui Kai, Ka-Leung Wong, and Peter A. Tanner**

An overview of some key points in persistent luminescence (PersL) is provided with an emphasis on tunneling phenomena. Notably, key experimental criteria are provided that can substantiate the occurrence of thermal and athermal tunneling and localized transitions. These are elucidated by reference to a Case Study and to some other relevant works. Many experimental studies of PersL have assigned the mechanism to be tunneling on the basis of the linear relationship of PersL decay between intensity, I, and time, t^{-k}, where k is a constant, or I^{-1} versus t. However, this relation also applies to the case where there is a uniform distribution of trap levels, which may be evident from the breadth of the TL peak. The key measurement for the assignment of below-conduction band processes is the absence of thermal conductivity.

1. Introduction

We focus on solid-state inorganic dielectric materials or semiconductors, which have a gap between the valence band (VB) and conduction band (CB). Luminescence refers to the emission of photons following an excitation process, often by irradiating the substance with light. The lifetime of emission (i.e., the time to reach 1/e of the initial intensity) depends upon the mechanism of radiation-material interaction and can range from ns to s. However, a much longer duration of up to many hours for the emission occurs in persistent luminescence (PersL) phenomena. Materials are usually charged by radiation and the energy is stored in traps. Several books and review articles concerning PersL are available in the literature.[1] This ability of a phosphor to emit light continuously for minutes, hours, or days after ceasing the excitation has aroused scientific interest due to its potential applications in many fields, including night vision, anti-counterfeiting, data encryption, data storage, bio-imaging, and biosensing, **Figure 1**.[2] Usually, PersL is preceded by bandgap excitation to form the electrons and holes which are then stored. This Perspective gives a non-mathematical account of other mechanisms of sub-bandgap excitation. In particular, the mechanism of PersL called tunneling is clarified, in order to identify and distinguish it by experiment. Although important equations and their derivations have been omitted, references are provided for their locations. The need for the Perspective is evident because the phenomenon of tunneling is often cited in current literature without sufficient experimental proof. Some background of PersL is first introduced.

H.-Y. Kai, K.-L. Wong, P. A. Tanner
Department of Applied Biology and Chemical Technology
The Hong Kong Polytechnic University
Hong Kong SAR, P. R. China
E-mail: klgwong@polyu.edu.hk; monkey.tanner@polyu.edu.hk, peter.a.tanner@gmail.com

The ORCID identification number(s) for the author(s) of this article can be found under https://doi.org/10.1002/adom.202500793

DOI: 10.1002/adom.202500793

2. General Introduction to Persistent Luminescence

Usually, the material is charged by a suitable radiation wavelength, or by ionizing radiation/particles, so that energy (electrons and holes) is stored in defects (traps) inside the material, **Figure 2a**. Commonly, the energy is released as photons at a recombination center when sufficient external energy has been delivered by light (optically stimulated luminescence, OSL) or thermal energy (thermally stimulated luminescence, TL), to recombine the electrons and holes. This detrapping process in Figure 2b involves delocalized electron transfer via the CB so that the energy from the recombination of charge carriers is conveyed nonradiatively to the center. The trap density determines the overall PersL intensity whereas the trap depth from the CB determines the duration of PersL. The probability s^{-1} for the release of a charge carrier at a trap increases with increasing temperature. Figure 2c shows an alternative, above VB, process of charging where a transition metal ion such as Mn^{2+} undergoes a metal–metal charge transfer (CT) excitation to the CB, also creating electrons and holes. The experimental study of PersL enables the determination of the parameters of traps such as the thermal depth, the frequency factor, and the order of kinetics, that determine their effect upon emission.

Alternative recombination methods that do not involve the CB are displayed in Figure 2d–f. In tunneling, a trap and a recombination center are faced by a barrier. The electron does not surmount the barrier, but tunnels through, according to a quantum mechanical effect. The first recombination method (Figure 2d) involves direct trap ground electronic state–recombination center transfer by tunneling,[1a] whereas the second method (Figure 2e) involves thermally assisted tunneling from a trap excited electronic state.[3] Tunneling recombination depends upon the energetic height of the tunnel barrier, shown in the figure as coincident with the recombination center for athermal tunneling, Figure 2d.[3b,c] For athermal tunneling, the PersL signal intensity and decay rate are independent of temperature. This is seldom tested experimentally.

Figure 1. Some applications of persistent luminescence.

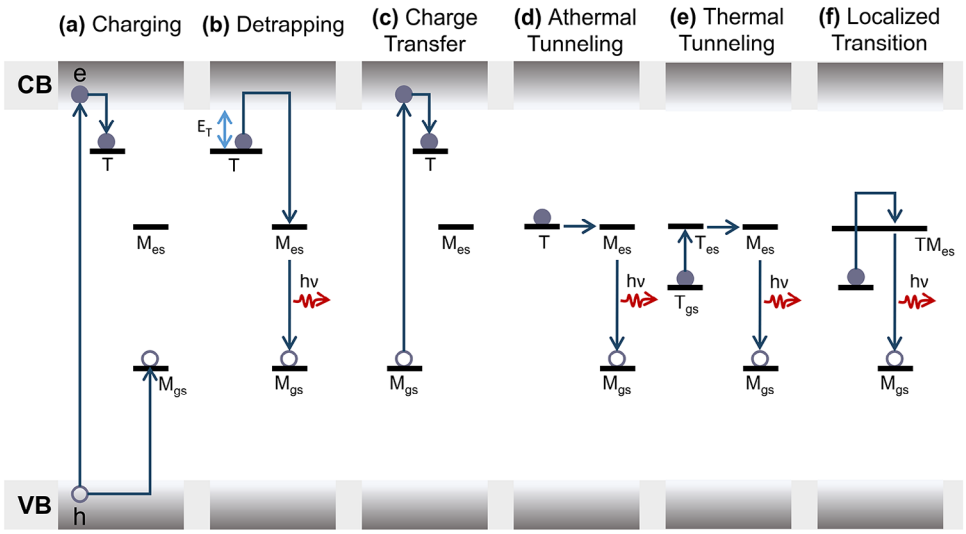

Figure 2. Some mechanisms of persistent luminescence. a) Irradiation energy greater than that of the bandgap is provided to excite electrons to the conduction band, leaving holes behind. The diffusion of these free carriers in the lattice occurs until they are trapped at defects (traps). b) At a certain temperature, sufficient thermal energy (activation energy) is available to excite electrons from the trap up to the CB (detrapping) and enable electron-hole recombination at the activator site, leading to photon emission. c) Above VB excitation by MMCT for the creation of electrons and holes. d) Athermal tunneling between the trap and recombination center, leads to photon emission. e) Thermally assisted tunneling from the trap excited state to the recombination center, leading to photon emission. f) Localized recombination involving jumping the barrier of the shared excited state. VB valence band, CB conduction band; e electron, h hole; T trap; M activator ion; gs, es ground and excited electronic state.

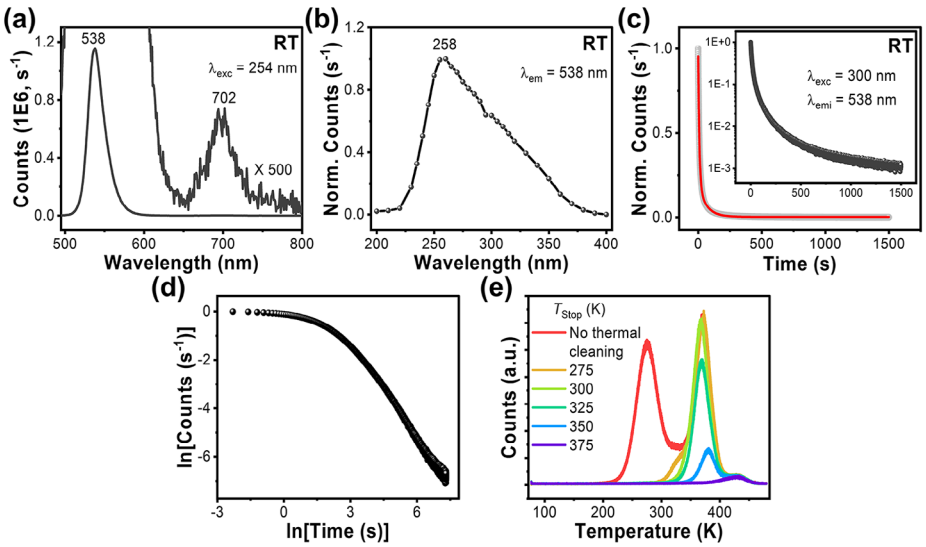

Figure 3. a) PersL spectrum of $Mg_{1.99}Mn_{0.01}La_3Sb_3O_{14}$ after bleaching at 480 K and then charging by 254 nm radiation at RT for 600 s. b) PersL excitation spectrum was obtained by monitoring intensity at 538 nm in repeated charging cycles using different wavelengths. PersL decay plotted on (c) linear (inset log) and d) ln–ln scales. The biexponential fit to (c) is shown in red: $\tau_1 = 9.3$ s, $\tau_2 = 63.9$ s; and the slope in (d) approaches -1.3 at later times. e) TL glow curves using the T_{STOP} technique with a linear heating rate of 7 °C min^{-1}. In each T_{STOP} experiment, the sample was cleaned at 480 K before the measurements and then irradiated at 77 K for 600 s. The sample was then heated to the appropriate T_{STOP} temperature before recording the TL.

As Vedda and Fasoli[1a] have pointed out, recombination can occur within a defect cluster: the electron and the hole are trapped within the same complex defect. Figure 2f displays this type of localized transition, where thermal excitation enables the shared excited state of the trap and recombination center (trap-M) to be achieved followed by photon emission.[4] In Figure 2d–f, the recombination frequency depends upon the distance between the separated charges. This means that nearby traps to the recombination center are involved, whereas the trap–recombination center distance is immaterial for recombination via the CB (Figure 2b). Also notice in Figure 2d–f that if sufficient thermal energy is available, electrons can also be excited from the trap into the CB level so that a mixture of localized and delocalized recombination can occur. This is an important point because the nearby trap population involved in tunneling will become depleted whereas CB recombination involving more distant traps can continue. The outcome of radiative recombination is that photons are emitted at the recombination site, which is often an ion such as Cr^{3+}, Mn^{2+}, or Eu^{2+}.

If the temperature of the sample is increased at a fixed heating rate, when sufficient energy E_T is provided, the detrapping gives a peak in the thermally stimulated luminescence (TL) plot of emission intensity versus temperature (called a glow curve), with maximum intensity at temperature T_m. The TL signal is proportional to the derivative of the concentration of charge carriers in certain traps. The TL peak can be analyzed based on its heating rate, shape, or area according to well-documented methods.[1c,d] A simple model for TL and the isothermal decay of PersL (often called the afterglow) employs general order kinetics to fit experimental data.[1d] The general order kinetics model employs one trap and one recombination center and assumes an unequal probability of retrapping and recombination with a center.

Typical results of Figure 2a–c, but generally illustrative, are displayed in **Figure 3**. Figure 3a displays the PersL spectrum of $Mg_{1.99}Mn_{0.01}La_3Sb_3O_{14}$ phosphor after irradiation by 254 nm UV light, involving the mechanisms in Figure 2a,c. The strong green Mn^{2+} PersL emission at 538 nm dominates Mn^{4+} emission ≈700 nm. The PersL excitation spectrum, Figure 3b, is recorded by monitoring the intensity of PersL at different irradiation wavelengths. The decay of the PersL can be monitored at a fixed temperature for a certain time period. The decay is shown on linear (Figure 3c) and logarithmic (Figure 3d) scales. Stable traps with depths E_T in the range 0.4–1.0 eV and lifetimes of several hours are generally suitable in PersL phosphors. The TL glow curves using the T_{STOP} technique[1b] (explained in the Section S2, Supporting Information), when monitoring 538 nm emission, are displayed in Figure 3e. TL peaks should ideally be corrected for temperature quenching[1e] and their shape conveys information concerning the recombination mechanism.[1b–d,f]

At the low-temperature range of a TL peak (up to ≈10% of the peak intensity), the intensity (I) is approximately proportional to $\exp(-E_T/kT)$. Hence, one simple way of determining the activation energy E_T is to plot $\ln(I)$ as a function of $1/T$ to produce a straight line with slope–E_T/k (Section S3, Supporting Information). Other methods of finding E_T involve the general order or general mixed order models.[5]

Various quantitative models have been proposed to explain TL and OSL results, and a summary has been given by McKeever and Chen and the reader is referred to this work.[4b]

3. Uniform Distribution of Trap Levels

The concept of one stable trap and one recombination center may not be realistic, however.[6] The thermal cleaning technique, in which the sample is heated to a temperature T_{STOP} after the

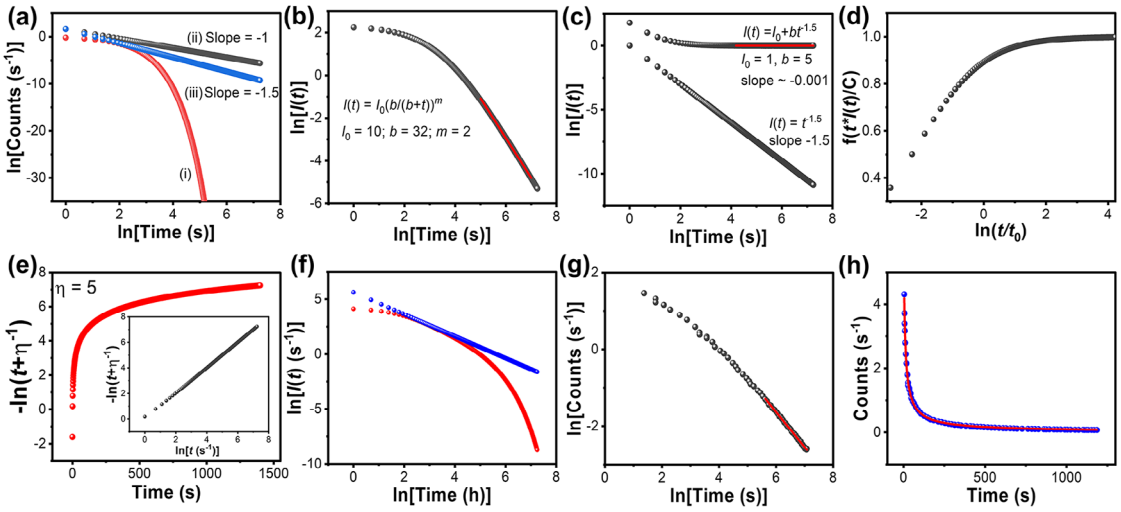

Figure 4. Characteristic decay curves. a) Equations (1) and (2), all on natural logarithm scale: (i) monoexponential decay; (ii) Equation (1); (iii) Equation (2) with $\alpha kT = 0.5$. b) Equation (3), the slope between abscissa values of 5 to 7 is −1.860±0.001. c) power law, t^{-k} time dependence, $k = 1.5$. d) Equation (4). e) Equation (6) on natural logarithm scale for ordinate (red) and for both abscissa and ordinate (black). f) Equation (7) on natural logarithm scale (red). The blue line shows the power relationship t^{-1} for tunneling. g) Plot of ln[Counts] versus ln[time] for the persistent luminescence decay of $ZnGa_2O_4:Cr^{3+}$ (0.25 at.%) excited by 550 nm radiation. (Adapted from ref. [25b] with Counts in arbitrary units). The slope of the linear fit in red is −0.91. h) The fit of data from Figure 4g to Equation (3) using three parameters, with $m = 0.82\pm0.02$, $R_{adj}{}^2 = 0.9980$.

excitation and before the TL experiment, is useful in investigating a trap depth distribution (Figure 3e).[1d] Many other scenarios are possible and have been modeled, such as retrapping the charge carriers by other traps with different activation energies and the presence of a continuous distribution of traps around a certain mean value.[7] Wu et al.[5] have argued that both scenarios would lead to a shift in the TL peak with longer delay times between charging and the TL experiment. The former could lead to a spread of emission over a wider temperature range, whilst for the latter, the half-width of the TL peak should decrease for longer delay times. The latter scenario, a continuous distribution of traps, is now considered in more detail.

Randall and Wilkins considered the thermal excitation of a set of identical traps and from a distribution of traps.[6] From their theory, the monoexponential decay equation is appropriate for a single trap depth (**Figure** 4a(i)). With some assumptions, this is modified for the case of a uniform distribution of trap energy levels (i.e., an equal number of traps at all depths), Figure 4a(ii):[6b,c]

$$I(t) = nkT/t\left(1 - e^{-st}\right) \sim nkT/t \rightarrow when\ st >> 1 \quad (1)$$

where $I(t)$ is PersL intensity at time t, T is temperature, n is the initial population of the trap distribution, k is the Boltzmann constant, and s is the frequency factor, also called the attempt-to-escape frequency factor.

For an exponential trap distribution:[6b,c]

$$I(t) = Bt^{-(\alpha kT+1)} \quad (2)$$

where the constant B has a weak temperature dependence and α is a constant. When $\alpha kT = 1$, an inverse square law results (Figure 4a(iii)).

Medlin[7a] assumed a Gaussian distribution of filled traps. In this case, the intensity of the glow peak at time t is approximated by:

$$I(t) = I_0\left(b/(t+b)\right)^m \quad (3)$$

where b (depending upon temperature) and m (depending upon the fraction of initially filled traps) are parameters for which the functional relations have been given. This relation is shown in Figure 4b for $m = 2$ and a linear portion (slope −1.86) follows an initial curve.

Other types of distribution[7b] were considered by other authors but the key point is that the PersL intensity exhibits an eventual inverse power law dependence upon time. Note that if a distribution of trap levels does exist, it should directly be shown as an anomalous broad linewidth in the TL peak. This can be observed by running TL curves at different starting temperatures after thermal cleaning (T_{STOP} method).

4. Tunneling Recombination

4.1. Athermal Tunneling

Tunneling-assisted recombination mechanisms have been shown in Figure 2d,e. Early studies that suggested carrier tunneling as a recombination mechanism include Dexter[8] for F-center electrons to positive hole centers; Delbecq et al. for M^0-Cl_2^- pairs in KCl:AgCl,[9] and Riehl's donor-acceptor model for the afterglow of ZnS:Cu at 6 K, where black body radiation was carefully excluded.[10] It has been assumed that the recombination center and trap are in close proximity for tunneling and the wavefunctions overlap.[1b] However, Dexter[8] argued that tunneling could occur over distances as long as 30–40 Å.

Some properties of athermal tunneling are itemized in the box.

The probability per unit time for tunneling between a discrete donor–acceptor pair follows first-order kinetics. The deviation of PersL decay signal in tunneling from first-order kinetics has been attributed to contributions from trap-recombination pairs at different distances and times from the start of irradiation.

For a random distribution of recombination centers, Huntley[16] proposed a model of athermal tunneling which assumes that the concentration of traps is much lower compared to recombination centers and that the tunneling of an electron occurs from a trap to the nearest recombination center only. No assumption is required about the distribution of traps. The

Important properties of athermal tunneling, Figure 2d

(i) TL due to tunneling and localized transitions is not accompanied by thermally stimulated conductivity (TC) of TL, contrary to processes involving the CB.

(ii) There is a fading of the TL signal for a delay time between irradiation and TL measurement; an anomalous heating rate dependence of the TL signal when competitive recombination processes occur.[11]

(iii) A power law t^{-k} time dependence occurs for the isothermal tunnelling recombination luminescence, Figure 4c (but see an alternative explanation for this law below).

(iv) A non-zero temperature-independent luminescence intensity is observed at low temperature in contradiction with the usual zero value.[12]

(v) The isothermal decay rate is the same for different temperatures.

(vi) A plot of TL remaining after anomalous fading against logarithm of storage time should be linear.[4b,12,13]

Thermally assisted tunneling, Figure 2e

(i)-(iii) as above.

(a) The excited state population of the trap increases with temperature according to Boltzmann equilibrium so that the afterglow lifetime decreases.[14]

(b) The activation energy of different traps is constant, but the frequency factor differs.[3a,14,15]

(c) The unique traps lead to monoexponential decay of PersL.[3a, 14-15]

Localized transition, Figure 2f

(i)-(iii) as above.

(d) The PersL emission spectrum exhibits new feature(s) associated with the trap-metal ion shared excited state.

power law of the form intensity $I \propto t^{-k}$ results, where t is time and k is a constant which is usually between 1 and 1.5, but can be less than 1 and as high as 2 (Figure 4c). The proportionality constant, s, is defined in Equation (1). The index k increases with increasing density of recombination centers.[16a]

It has been assumed in item (iii) in the box that the duration of charging is infinitely short. However, it is usual that the values of $tI(t)$ are not constant during the initial stage of afterglow ($I(t) \sim C/t$ only if $t>>t_0$ where t_0 is the irradiation length) because ion pairs are created at a constant rate and can decay during the time interval $-t_0<t<0$. Hence the appropriate equation is:[4b,9]

$$tI(t) = C\left[\frac{t}{t_0}\right]\ln\left(1+\frac{t_0}{t}\right) \quad (4)$$

The graph of $tI(t)/C$ versus t/t_0 exhibits an increase from the initial value and asymptotically approaches the value 1,[9] (Figure 4d).

Alternatively given for long-range tunneling of polymers:[16b]

$$I(t) = I_0/(1+\alpha t)^m \quad (5)$$

which is effectively the same as Equation (3).

4.2. Thermally Assisted Tunneling

Several alternative scenarios have been given for thermally assisted tunneling recombination. First, it is envisaged that thermal assistance to a vibrationally-excited trap state occurs, from which athermal tunneling occurs to an excited state of the recombination center.[1a] On the other hand, the model of Dobrowolska et al.[17] includes a trapped electron having a triangular barrier with the recombination center excited state, for which the width decreases with the higher energy of the electron. The electron tunnels through the barrier to an excited state of the acceptor. In all cases, wavefunction overlap occurs and this involves proximity of the donor and acceptor, often as a nearest-neighbor pair.

The OSL decay for thermally assisted tunneling, Figure 2e, involving a single donor-acceptor pair should be governed by first-order kinetics. The thermal dependence of tunneling blurs the distinction between the occurrence of a trap distribution and thermally assisted tunneling but T_{STOP} measurements or fading experiments[18] (see below) can help to resolve this.

A general equation for luminescence (photon counts s^{-1}) from thermally stimulated tunneling was given by Avouris and Morgan[3b] when considering a distribution of donor–acceptor pairs, Figure 4e:[3b]

$$I(t) = 1/\left(t+\eta^{-1}\right) \; for\; \eta t >> 1 \quad (6)$$

where $I(t)$ is the intensity at time t and η is a defined constant that does not include temperature. These authors commented that "TL involves detrapping by thermal activation and it has been shown that a distribution of traps gives a t^{-1} decay; however, in a photostimulated PersL experiment, the detrapping rate is determined by the light intensity, so that a t^{-1} dependence cannot be explained by a distribution of traps". Although Equation (6) may be applicable, we question the conclusion in the case of Avouris and Morgan's study of Zn_2SiO_4:Mn^{2+} that electron tunneling occurs. The wavelength of 254 nm was employed and it leads to metal-metal charge transfer for Mn^{2+}[19] so that an electron is excited to the CB and the recombination is not by tunneling. Indeed, it was shown from the TL results[3b] that a distribution of traps is present in this system, and later that the conduction band is involved in the PersL process.[20]

4.3. Localized Transitions

The thermally assisted localized model does not involve tunneling but suggests that the trapped electron hops over the barrier of the shared excited state with the acceptor (Figure 2f). Templer[4a] described the situation where the donor is not a single trap but a distribution of trap levels with energies between E_{max} and E_{min} below the thermal barrier. In this case, the intensity of PersL is given by Figure 4f:

$$I(t) = \left(n_0 kT/t\right) \times \left[\exp\left(-t/\tau_{max}\right) - \exp\left(-t/\tau_{min}\right)\right] \quad (7)$$

where n_0 represents the initial concentration of electrons per unit energy; t refers to the time elapsed after irradiation; and the τ are the characteristic lifetimes of traps situated at maximum and minimum depths below the CB. Trap sites that have a large separation from the recombination center can only recombine via the CB.

Mandowski[21] and others[22] have formulated models combining both localized and delocalized transitions and Land[23] has given equations for TL. The model of Jain et al.[24] is more general and includes the variation of the distribution of the trap–recombination center distances in space and time. It not only includes donor–acceptor recombination for a donor center having an excited state below the CB but also those systems where tunnelling occurs only through the ground state.

5. Comments

It is clear that a necessary criterion for assigning athermal or thermally assisted tunneling or localized recombination is the absence of electric current flow during the process. The variety of equations put forward in various studies appears to be confusing. However, observation of t^{-k} decay is not sufficient proof of tunneling. Also, the distinction between the distribution of trap levels and athermal tunneling may partly involve the temperature dependence of PersL decay, besides TL behavior. Furthermore, we understand that athermal tunneling leads to a TL baseline displacement independent of temperature, whereas a broad TL peak results from a distribution of traps. It is important to carry out isothermal decay experiments at different temperatures to rule out the second scenario of thermally assisted tunneling (see later). The comparison between decays at the same temperature but following different heating cycles also may be useful.[1a] Experimental verification of thermally assisted tunneling may not be straightforward, even when doping with different luminescent ions and checking the modification of the peak shape and temperature position.[1a] The study of Vedda et al.[3a] provides more secure proof of thermally assisted tunneling since the same set of

traps is involved for different TL peaks, with different frequency factors (see later). This differs from the case study below, where a continuous distribution of traps is involved.

We propose a signature for the recombination mechanism. Since the shared electronic state of the metal ion and trap differs from that of the metal ion alone, the emission spectra should also differ. This is found to be the case, for example, for $ZnGa_2O_4:Cr^{3+}$, for which PersL is achieved using sub-bandgap excitation.[25] The emission spectrum comprises a defect peak labeled Cr_{N2} which distinguishes the shared excited state from the Cr^{3+} excited state. The mechanism for PersL has been proposed to involve the antisite defect $Zn'_{Ga} - Cr_{N2} - Ga^{\times}_{Zn}$ clusters. The 298 K OSL decay for 0.25% Cr^{3+} doping, after 550 nm excitation, is shown in Figure 4g. The decay is not monoexponential. Also, we are unable to fit the graph using Equation (7). In view of the emission spectrum, we associate the mechanism with localized recombination, and the fit with Equation (3) in Figure 4h shows that there may also be a distribution of traps.

6. Anomalous Fading

Normal fading, a reduction of the TL signal with time, may occur when the charged sample is held at a temperature lower than that of the TL peak. However, in the case of anomalous fading, the signal decays quite fast when the sample is held at a significantly lower temperature. This is a consequence and a signature of athermal tunneling (or an alternative)[26] since the number of trapped electrons diminishes with time after the irradiation of the sample has ceased. Hence there is a fading of the subsequent TL signal: a longer delay between irradiation and heating to record the glow curve gives a weaker TL signal. This anomalous fading, involving the unexpected loss of charge carriers responsible for high temperature TL therefore has unwanted consequences for TL dating of minerals. Note that an apparent anomalous fading may be due to the occurrence of a very narrow TL peak, because of radiationless transitions to competing recombination centers.[27]

7. Case Study

Dobrowolska et al.[17] and Bos et al.[28] have investigated (thermally assisted) electron tunneling from a Ln^{2+} (Ln = Er, Nd, Ho, Dy) electron trap to a Ce^{4+} (= Ce^{3+}+h) recombination center in $YPO_4:Ce^{3+}$, Ln^{3+}. Here, we present the major experimental results of this important work. **Figure 5a** shows the TL of a sample with Ln = Dy after beta irradiation. We note that our group was unable to obtain TL when exciting $YPO_4:Ce^{3+}$ and Dy^{3+} using UV radiation, which emphasizes the requirement to produce Dy^{2+} ions. Peaks 1, 2, and 3 in Figure 5a represent recombination via the CB whereas the broad area 4 is due to tunneling from the trap Dy^{2+} to the recombination center Ce^{4+} (Figure 5b). The glow curves recorded immediately after irradiation, and those with a 2 h delay, differ with respect to an elevated baseline background in the first case. This first scenario represents tunneling and CB recombination, whereas the nearby traps have been depleted in the second case so that recombination only occurs via the CB from distant traps. The broad baseline background increases when the Ce and Dy concentration is increased.

The TL curves were recorded by Dobrowolska et al. at different delay times after irradiation at 150 and 300 K. The integrated area of the TL glow peak decreased when the delay time increased, showing fading behavior. The fading rate increased with the Ce and Dy concentration and with temperature, showing thermal assistance.

The Ce^{3+} emission at $T = 150$ K for YPO_4:Ce, Dy (where the lanthanide ions are each at the concentration of 2 at.%) was almost entirely due to tunneling recombination. The isothermal decay curve could be fitted by the power law: Intensity $\alpha\ t^{-0.25}$. There was an initial deviation from the fit and this was attributed by the authors to concentration-induced nonradiative processes or experimental error. We have noted above that the initial period does not conform to the simple power law. The power index was found to change with concentration and temperature. The decay was not monoexponential because it resulted from a distribution of distances between the trap and the recombination center.

The dependence of the TL glow curve upon the heating rate was investigated for two different Ln concentrations in YPO_4:Ce,

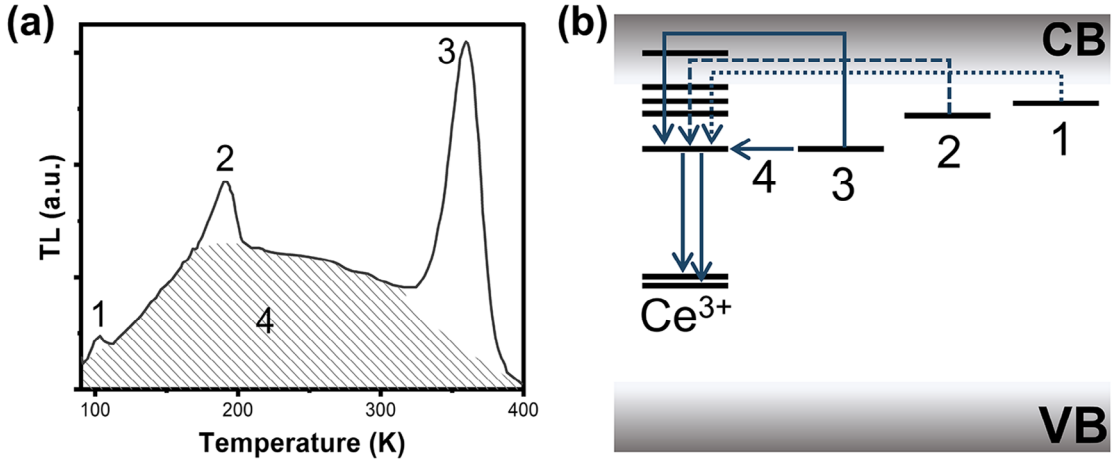

Figure 5. a) Low-temperature TL of YPO_4: Ce, Dy measured after β^- irradiation with a heating rate of 0.5 K s^{-1}. The concentrations of Ce^{3+} and Dy^{3+} are each 5 at.%. The shaded part is attributed to tunneling recombination. b) A schematic of the different recombination pathways. (Reproduced from ref. [17] with permission).

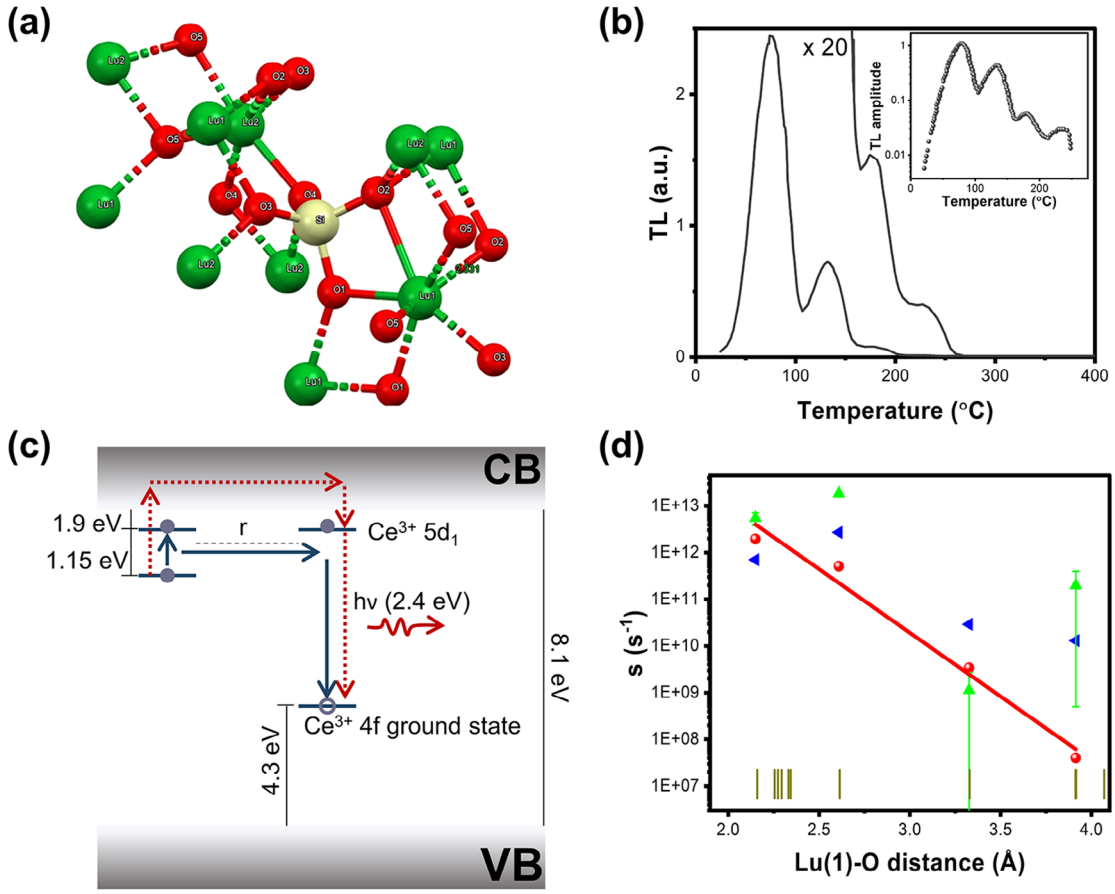

Figure 6. a) Structure of Lu_2SiO_5 crystals, showing the two Lu sites. b) TL of Lu_2SiO_5:Ce. The inset shows the glow curve (on a log scale) corrected for the thermal decay of the Ce^{3+} 5d-4f transition. c) Valence band-conduction band diagram representing thermally assisted tunneling in Lu_2SiO_5:Ce. The band gap is from ref. [34]. The ground state of Ce^{3+} is estimated from Figure 7 in ref. [35] and the lowest $5d^1$ level is from the overlap of excitation and emission spectra.[36] d) Frequency factors of the TL peaks of Lu_2SiO_5:Ce versus the nearest O–Ce distances, taken as Lu(1)–O distances (red circles, as in ref. [3a]). The red line is the monoexponential fit performed on the data in ref. [3a]. Blue triangles from ref. [15] green triangles from ref. [14]. The brown vertical lines in d represent our measurements of Lu(1)–O distances from the crystal structure[32] using the software, Diamond. (b reproduced from ref. [3a] with permission).

Dy (each 0.5 at.%, and each 5%). In the first case, the glow peak height decreased with increasing heating rate, following first-order kinetics.[1d] However, at the higher concentration, the glow peak intensity increased with the heating rate. The authors[17] presented a simple model with a square trap separated by a triangular potential barrier from the excited state of the Ce^{4+} ion, based upon certain assumptions, in order to account for the experimental observations. The model shows that the distance between the trapped electron (Dy^{2+}) and the recombination center (Ce^{4+}) affects the tunneling luminescence much more than other factors, such as temperature or trap depth. The interested reader is referred to this work.

8. Some Previous Studies Ascribed to PersL Tunneling

The PersL of rare earth silicate systems has been intensively studied. Blahuta et al.[15] provided proof that the defects responsible for the main TL peaks in Lu_2SiO_5:Ce^{3+} crystals (**Figure 6a**) are oxygen vacancies. Yamaga et al.[29] displayed PersL decay curves at 300 and 500 K for this system and showed that they do not fit to a single exponential function, but to $t^{-0.2}$ and t^{-1} power functions, respectively. Vedda and co-workers[3a,30] have associated several TL peaks (1–4 in Figure 6b) with just one type of trap defect which undergoes thermally assisted tunneling. The argument given was that the activation energy, E_T, is the same for each TL peak but the frequency factor varies in a monoexponential fashion with the bond distance of the trap from the recombination center. This scenario is shown in Figure 6c for Lu_2SiO_5:Ce^{3+} crystals. In this system, the four glow peaks between ≈350 and ≈510 K are observed due to Ce^{3+} $5d^1 \rightarrow 4f^1$ emission and were assigned by Vedda et al.[3a] to thermally assisted tunneling because no TC signal was observed in each case. The trap depths were measured by the initial rise method and the frequency factor, s, from first-order recombination kinetics using different heating rates, β (°C s^{-1}):

$$s = \frac{\beta E_T}{kT_m^2} \exp\left(\frac{E_T}{kT_m}\right) \tag{8}$$

Table 1. TL peak maxima, T_m (K), activation energy, E_T (eV), and frequency factor, s (s^{-1}), for Lu_2SiO_5 scintillators.

System Ref. [14]	T_m	E_T	s	System Ref. [15]	T_m	E_T	s	System Ref. [3a]	T_m	E_T	s
					49						
					140						
					182						
[a]	338	0.97	5.47E12	[b]	354	0.95	7.0E11	[a]	351	1.0	1.95E12
0.25 at.% Ce	391	1.17	1.82E13	0.22 at% Ce	410	1.14	2.7E12	0.04 at.% Ce	408	1.0	5.08E11
	467	0.95	1.13E9		464	1.12	2.9E10		454	1.0	3.40E9
	547	1.30	1.97E11		526	1.24	1.3E10		509	1.0	4.0E7
	611				558	1.7	4.8E13				

[a] Lu_2SiO_5; [b] $Lu_{1.798}Y_{0.1998}SiO_5$.

where k is the Boltzmann constant and T_m is the peak maximum in TL. The oxygen vacancy traps were assumed to be at different distances from the cerium recombination center. The comparisons of the peak maxima, activation energies, and frequency factors with two other studies are given in **Table 1**.

Electron spin resonance and theoretical studies show that Ce^{3+} almost exclusively occupies the larger (7-coordinate) Lu site in Lu_2SiO_5.[31] The distances from this site, Lu(1), Figure 6a, to oxygen atoms (i.e., the O_v) were calculated by Vedda et al. from the crystal structure with some averaging.[3a] The TL peaks between 351 and 509 K were then associated with the same trap depth, 1 eV. Figure 6d displays the plot of the determined frequency factors of these TL peaks against O-Lu(1) distances, representing the oxygen vacancy–cerium distances. The red circles and the red fitted line are from ref. [3a]. There have been other studies of the PL and PersL of this system due to interest in its application as a scintillator, and the data of Blahuta et al.[15] and Dorenbos et al.[14] are also included in the figure and given in Table 1. Within the figure, the vertical brown bars represent our measurements of Lu(1)—O bond distances from the software Diamond using the crystal structure of Lu_2SiO_5.[32] The values are similar to those employed by Vedda et al. It would be expected that an oxygen vacancy next to Ce^{3+} would reduce the ionic radius, but the contraction would be similar for more distant neighbors. Since the intensity of the TL peak is partly dependent upon the trap population, as well as the frequency factor, the much higher value for the peak at 345±6 K is evident. There are some discrepancies in the values of s and ET in Table 1, but Vedda et al.[3a] have provided strong evidence for their explanation of the TL peaks. The reason for the absence of peaks corresponding to Ce^{3+}-O_v distances of 2.2–2.3 Å (Figure 6d) is unclear unless they are hidden in the wings of the major TL peak. Vedda et al. did not investigate the PersL decay. For specific recombination centers (i.e., h-Ce^{3+}-O_v at fixed sites) it would be expected that the afterglow is monoexponential. This was in fact found by Dorenbos et al.[14] for the first 3 h after illumination and seeks to strengthen the interpretation of Vedda et al.

The more recent first principles study[31c] shows that the formation of Ca_{Lu}-V_O complex defects is favored in Lu_2SiO_5:Ce co-doped with Ca.

Interestingly, the scenario of TL peaks due to a fixed trap depth and different frequency factors for neighbors has not been discovered in other systems, for example, in LuAG:Ce^{3+}, where a recombination center of the type Lu_{Al}-Ce^{3+}-O_v has been suggested, together with thermally assisted tunneling between 10 and 100 K, but giving a PersL decay of the type Equation (3).[33]

9. Take Home Message

Table S1 (Supporting Information), summarizes a random assortment of studies in which tunneling PersL has been suggested and provides the reasoning given in each case in the final column. The sole criterion in many of these works is the occurrence of a power law for PersL decay. Since such a power law variation also occurs for a continuous distribution of trap energy levels, it could be appropriate to investigate further by reference to Box 1. This has seldom been done and Reviewers have not pointed this out.

The uniqueness of the tunneling and localized transition models lies in the below CB mechanisms and the absence of TC. However, the mechanism of PersL is unclear in many cases and may involve several scenarios. The ability to distinguish between tunneling and a localized transition is argued in refs. [S19] and [S20] in Table S1 (Supporting Information). With more careful studies, such as these two, the future holds promise for a more detailed understanding of PersL mechanisms.

Supporting Information

Supporting Information is available from the Wiley Online Library or from the author.

Acknowledgements

K.-L.W. acknowledges financial assistance from the Hong Kong Research Grants Council No. 12300021 and NSFC/RGC Joint Research Scheme (N_PolyU209/21). The authors are indebted to Dr. Waygen Thor for reading the manuscript and providing comments.

Conflict of Interest

The authors declare no conflict of interest.

Author Contributions

H.-Y.K.did investigation, review & editing. K.-L.W. did funding acquisition. P.A.T. did review & editing.

Keywords

afterglow, fading, localized transition, persistent luminescence, thermoluminescence

Received: March 11, 2025
Revised: March 29, 2025
Published online: June 14, 2025

[1] a) A. Vedda, M. Fasoli, *Radiat. Meas.* **2018**, *118*, 86; b) R. Chen, S. W. S. McKeever, in *Theory of Thermoluminescence and Related Phenomena*, World Scientific, Singapore, Singapore **1997**; c) V. Pagonis, G. Kitis, C. Furetta, in *Numerical and Practical Exercises in Thermoluminescence*, Springer Science & Business Media, Berlin, Germany **2006**; d) S. W. S. McKeever, in *Thermoluminescence of Solids*, Cambridge University Press, Cambridge, UK **1985**, *3*; e) D. Van der Heggen, D. Vandenberghe, N. K. Moayed, J. De Grave, P. F. Smet, J. J. Joos, *J. Lumin.* **2020**, *226*, 117496; f) R. Chen, Y. Kirsh, in *Analysis of Thermally Stimulated Processes*, Elsevier Science & Technology Books, Amsterdam, The Netherlands **1981**; g) Y. Kirsh, *Phys. Status Solidi.* **1992**, *129*, 15.

[2] a) S. Shionoya, W. M. Yen, H. Yamamoto, in *Phosphor Handbook*, CRC Press, Boca Raton, FL, USA **2018**; b) D. Poelman, D. Van der Heggen, J. Du, E. Cosaert, P. F. Smet, *J. Appl. Phys.* **2020**, *128*, 240903; c) Y. Zhuang, L. Wang, Y. Lv, T.-L. Zhou, R.-J. Xie, *Adv. Funct. Mater.* **2018**, *28*, 1705769; d) J. Yang, Y. Zhou, H. Ming, E. Song, Q. Zhang, *ACS Appl. Electron. Mater.* **2022**, *4*, 831; e) A. Abdukayum, J.-T. Chen, Q. Zhao, X.-P. Yan, *J. Am. Chem. Soc.* **2013**, *135*, 14125; f) S.-K. Sun, H.-F. Wang, X.-P. Yan, *Acc. Chem. Res.* **2018**, *51*, 1131.

[3] a) A. Vedda, M. Nikl, M. Fasoli, E. Mihokova, J. Pejchal, M. Dusek, G. Ren, C. R. Stanek, K. J. McClellan, D. D. Byler, *Phys. Rev. B–Condens. Matter Mater. Phys.* **2008**, *78*, 195123; b) P. Avouris, T. Morgan, *J. Chem. Phys.* **1981**, *74*, 4347; c) G. Kitis, V. Pagonis, *J. Lumin.* **2013**, *137*, 109.

[4] a) R. H. Templer, *Rad. Protect. Dosim.* **1986**, *17*, 493; b) S. W. S. McKeever, R. Chen, *Radiat. Meas.* **1997**, *27*, 625.

[5] H. Wu, Y. Hu, X. Wang, *Radiat. Meas.* **2011**, *46*, 591.

[6] a) A. J. J. Bos, *Radiat. Meas.* **2007**, *41*, S45; b) J. T. Randall, M. H. F. Wilkins, *Proc. R. Soc. Lond. A. Math. Phys. Sci.* **1945**, *184*, 347; c) J. T. Randall, M. H. F. Wilkins, *Proc. R. Soc. Lond. A. Math. Phys. Sci.* **1945**, *184*, 365.

[7] a) W. L. Medlin, *Phys. Rev.* **1961**, *123*, 502; b) K. Van den Eeckhout, A. J. J. Bos, D. Poelman, P. F. Smet, *Phys. Rev. B–Condens. Matter Mater. Phys.* **2013**, *87*, 45126.

[8] D. L. Dexter, *Phys. Rev.* **1954**, *93*, 985.

[9] C. J. Delbecq, Y. Toyozawa, P. Yuster, *Phys. Rev. B* **1974**, *9*, 4497.

[10] N. Riehl, *J. Lumin.* **1970**, *1*, 1.

[11] A. Mandowski, A. J. J. Bos, *Radiat. Meas.* **2011**, *46*, 1376.

[12] R. Visocekas, *Rad. Protect. Dosim.* **2002**, *100*, 45.

[13] J. Ueda, *Bull. Chem. Soc. Jpn.* **2021**, *94*, 2807.

[14] P. Dorenbos, C. W. E. Van Eijk, A. Bos, C. Melcher, *J. Phys.: Condens. Matter* **1994**, *6*, 4167.

[15] S. Blahuta, A. Bessière, B. Viana, V. Ouspenski, E. Mattmann, J. Lejay, D. Gourier, *Materials* **2011**, *4*, 1224.

[16] a) D. J. Huntley, *J. Phys.: Condens. Matter* **2006**, *18*, 1359; b) Y. Hama, Y. Kimura, M. Tsumura, N. Omi, *Chem. Phys.* **1980**, *53*, 115.

[17] A. Dobrowolska, A. J. J. Bos, P. Dorenbos, *J. Phys. D: Appl. Phys.* **2014**, *47*, 335301.

[18] O. Q. De Clercq, D. Poelman, *ECS J. Solid State Sci. Technol.* **2017**, *7*, R3171.

[19] P. Diana, D. Sivaganesh, V. Sivakumar, J. N. Gopal, S. Sebastian, S. Saravanakumar, *J. Mater. Sci.: Mater. Electron.* **2023**, *34*, 1992.

[20] I. F. Chang, P. Thioulouse, E. Mendez, E. Giess, D. Dove, T. Takamori, *J. Lumin.* **1981**, *24*, 313.

[21] A. Mandowski, *J. Phys. D: Appl. Phys.* **2004**, *38*, 17.

[22] a) M. Kumar, R. Kher, B. Bhatt, C. Sunta, *J. Phys. D: Appl. Phys.* **2006**, *39*, 2670; b) M. Kumar, R. Kher, B. Bhatt, C. Sunta, *J. Phys. D: Appl. Phys.* **2007**, *40*, 5865.

[23] P. L. Land, *J. Phys. Chem. Solids* **1969**, *30*, 1693.

[24] M. Jain, B. Guralnik, M. T. Andersen, *J. Phys.: Condens. Matter* **2012**, *24*, 385402.

[25] a) A. Bessière, S. K. Sharma, N. Basavaraju, K. R. Priolkar, L. Binet, B. Viana, A. J. J. Bos, T. Maldiney, C. Richard, D. Scherman, *Chem. Mater.* **2014**, *26*, 1365; b) S. K. Sharma, A. Bessière, N. Basavaraju, K. R. Priolkar, L. Binet, B. Viana, D. Gourier, *J. Lumin.* **2014**, *155*, 251.

[26] J. L. Lawless, R. Chen, V. Pagonis, *Radiat. Meas.* **2023**, *160*, 106881.

[27] R. Chen, P. L. Leung, M. J. Stokes, *Radiat. Meas.* **2000**, *32*, 505.

[28] A. J. J. Bos, P. Dorenbos, A. Bessière, A. Lecointre, M. Bedu, M. Bettinelli, F. Piccinelli, *Radiat. Meas.* **2011**, *46*, 1410.

[29] M. Yamaga, Y. Ohsumi, T. Nakayama, T. P. J. Han, *Opt. Mater. Express* **2012**, *2*, 413.

[30] a) A. Vedda, M. Martini, F. Meinardi, J. Chval, M. Dusek, J. Mares, E. Mihokova, M. Nikl, *Phys. Rev. B* **2000**, *61*, 8081; b) O. Sidletskiy, A. Vedda, M. Fasoli, S. Neicheva, A. Gektin, *Phys. Rev. Appl.* **2015**, *4*, 24009.

[31] a) L. Pidol, O. Guillot-Noël, A. Kahn-Harari, B. Viana, D. Pelenc, D. Gourier, *J. Phys. Chem. Solids* **2006**, *67*, 643; b) L. Ning, L. Lin, L. Li, C. Wu, C.-k. Duan, Y. Zhang, L. Seijo, *J. Mater. Chem.* **2012**, *22*, 13723; c) J. Cai, Y.-Y. Yeung, *Phys. Rev. B* **2023**, *107*, 85149.

[32] T. Gustafsson, M. Klintenberg, S. Derenzo, M. Weber, J. Thomas, *Cryst. Struct. Commun.* **2001**, *57*, 668.

[33] M. Nikl, A. Vedda, M. Fasoli, I. Fontana, V. Laguta, E. Mihokova, J. Pejchal, J. Rosa, K. Nejezchleb, *Phys. Rev. B–Condens. Matter Mater. Phys.* **2007**, *76*, 195121.

[34] M. Kitaura, S. Tanaka, M. Itoh, *J. Lumin.* **2015**, *158*, 226.

[35] P. Dorenbos, *Opt. Mater.* **2017**, *69*, 8.

[36] W. M. Yen, M. Raukas, S. A. Basun, W. Van Schaik, U. Happek, *J. Lumin.* **1996**, *69*, 287.